THE MODIFICATION AND MINIMIZATION OF SPINEL ($MgO{\cdot}Al_2O_3$) INCLUSIONS FORMED IN Ti ADDED STEEL MELTS

Seon-Hyo Kim & Chang-Woo Seo
Pohang University of Science and Technology, Korea

Sung-Koo Jo
Research Institute of Industrial Science & Technology, Korea

Min-Oh Suk & Sun-Min Byun
POSCO, Korea

ABSTRACT

The high melting point inclusions such as spinel ($MgO{\cdot}Al_2O_3$) could easily clog the SEN nozzle in a continuous caster mold. Especially, the Ti alloyed steels show severe nozzle clogging problem, resulting in worse slab surface quality. In this work, the thermodynamic role of Ti in steels and the effect of Ca treatment and Ti addition to molten austenitic stainless steel deoxidized with Al on the formation of spinel inclusions were investigated. Ca and Ti additions after Al deoxidation were performed in the order of Ca treatment → Ti alloying and vice versa. The inclusion chemistry and morphology according to those sequential orders are discussed from the standpoint of spinel formation.

The interaction parameters of Mg with respect to alloying elements were determined. Ti in steels could contribute to enhance the spinel formation, because Ti accelerates Mg dissolution from the MgO containing refractory walls or slags due to its high thermodynamic affinity for Mg ($e_{Mg}^{Ti} = -0.933$).

The samples were analyzed for determining the inclusions. The results are also discussed in the aspects of minimization of spinel inclusions. The optimum processing conditions for Ca treatment and Ti addition in austenitic STS melts to achieve the minimized spinel formation and maximized Ti yield will be proposed in this work, based on the inclusion chemistry and morphology according to the sequential charging orders as well as the thermodynamic behavior of Ti.

INTRODUCTION

A novel technology to control inclusion composition in steel was recently required, depending on the steel grade, strip thickness and /or surface finishing, as well as the pursuit of high cleanliness. Thus, the existence of a hard inclusion such as Spinel deteriorates the final quality of steel products because it has a high melting point and exists as a C-type inclusion [1], which is not plastically deformed and evenly dispersed. It also induces nozzle clogging, which decreases productivity and process effectiveness.

Therefore, a means of preventing and minimizing the occurrence of spinel formation in a given steel composition is requisite for the production of high-grade clean steels in stabilized processes.

Some studies to clarify the formation mechanism of spinel inclusion have been recently reported. Itoh *et al.* [2] studied inclusion compositions in liquid iron in a dolomite crucible deoxidized by Al. The experimental results agree with the phase stability diagram of spinel inclusion estimated from thermo-dynamical data. Ohta *et al.* [3] studied Ca-O and Mg-O equilibria in liquid iron with CaO-SiO_2-Al_2O_3-MgO slags at 1873 K using CaO or MgO crucibles. In their report, the phase stability regions in Fe-Al-Ca-O and Fe-Al-Mg-O systems estimated at 1873 K agreed with the experimental data. Some studies performed by Nishi [4] and Okuyama [5] focused on the effect of slag basicity on MgO content in inclusions in stainless steel, which resulted in a higher slag basicity. Kim *et al.* [6] reported that the spinel inclusion in the Type 304 stainless steel melt deoxidized by Al and Ti could be avoided with a decrease in both MgO content in an AOD slag and Al content in the melt.

From these previous investigations, [2, 3, 4, 5] a very small amount of Mg and Al (a couple of mass ppm) enables the formation of spinel inclusion in molten iron or steel that is deoxidized by Al.

Especially, the detection of spinel inclusion implies that attractive interaction between dissolved Ti and Mg component in slag or refractory in Ti added austenitic stainless steel deoxidized with Al. But, there have been only a few reports [7, 8, 9, 10] on the experimental determination of the interaction parameters between Mg and other element, as shown in Table 1. To ascertain the role of dissolved Ti in spinel formation, the equilibria between Mg vapor and third elements in liquid iron were investigated by Han [10] and Jo [11]. In this study, the vapor/liquid equilibration method [12] was applied to quantitatively determine the effect of a third element Ti on the behavior of Mg activity in liquid iron at 1873 K. The results will be discussed in regard to the thermodynamic potential to cause Mg dissolution into steel from slag or refractory materials and, finally, to facilitate spinel formation in steel.

The most general recognition is that calcium treatment [13, 14] is only a countermeasure to avoid harmful alumina or spinel inclusions, modifying them to harmless calcium aluminate inclusions. Calcium modification of Ti bearing inclusions in steel contributes to the production of high quality steel from the defects caused by inclusions, and to the prevention of nozzle blockage by inclusions build-up during casting. The results described in previous papers did not consider the effect of the order of Ca and Ti additions. In those experiments, Ti was first added and then calcium treatment was done. Harmful inclusions such as spinels could then be found in the steel.

Table 1: Summary of previous works on e^i_{Mg} in liquid iron

Authors	e^{Al}_{Mg}	e^{Cr}_{Mg}	e^{Ni}_{Mg}	e^{Ti}_{Mg}	e^{Si}_{Mg}	e^{C}_{Mg}
Sigworth and Elliott [7]	-	-	-	-	-	0.14
Nadif and Gatellier [8]	-	0.010	-0.012	-	-	-
Turkdogan [9]	-	-	-	-	-0.046	-0.15
Han [10]	-0.12	0.05	-0.03	-0.51	-0.09	-0.25
Jo [11]	-0.277	0.022	-0.033	-0.64	-0.096	-0.31

Therefore, to prevent and modify these deleterious inclusions, Ca and Ti additions after Al deoxidation were tested in the order of Ca treatment → Ti alloying and vice versa. The inclusion chemistry and morphology according to those sequential orders will be discussed from the standpoint of spinel formation.

METHODOLOGY

An equilibrium study between Mg vapor and liquid iron was carried out 1873 K in a $LaCrO_3$ resistance furnace with a fused alumina tube of 50-mm diameter and a hot zone length of 5 mm. A molybdenum reaction chamber with an iron cover was installed inside the tube. A schematic diagram of the experimental apparatus is shown elsewhere in detail [12].

The MgO crucible containing 10 g of high-purity electrolytic iron (99.99 pct) and an appropriate amount of Ti was positioned in the hot-temperature zone (1873 K) where the reaction temperature was controlled within an accuracy of ± 2 K. A MgO crucible containing Mg granules (99.9 pct) was then positioned in the lower-temperature zone and the liquid Mg temperature (T_{Mg}) was measured by a Ni/Cr_{10}-$Ni/Al_3/Si_3$ thermocouple embedded inside the iron cover. While reaching the desired reaction temperature, the molybdenum chamber was tightly sealed by an iron cover due to the effect of different thermal expansion coefficients. After holding the reaction for 5 hours, as confirmed in the previous work, [15, 16] the molybdenum chamber was taken out of the furnace and its lower part was quenched rapidly in ice water, whereas the upper part was quenched slowly in air so as to prevent Mg evolution from the iron melt during quenching.

For the inclusion study, a sample was melted by a 15 kW/50 kHz high frequency induction furnace shown in Figure 1. Four hundred grams of Fe-alloy (0.04 pct C, 0.6 pct Si, 1.4 pct Mn, 16.8 pct Cr, 10.7 pct Ni, 2.1 pct Mo) contained in a MgO crucible (OD: 45 mm, ID: 40 mm, H: 150 mm) together with an appropriate amount of $CaCO_3$-$MgCO_3$ mixture was melted at 1873 K. Temperature was measured by a thermocouple of Pt/6 pct Rh-Pt/30 pct Rh. The temperature reading of the thermocouple was connected to the PID controller of the induction furnace, hence to automatically adjust the power to keep the temperature of melt at 1873 K ± 10 K. After melting the Fe-alloy, an appropriate amount of Al (99.99 pct), Ca (99.5 pct) and Ti (99.99 pct), which were wrapped in Fe-foil and kept in a glass tube by magnets, were dropped into liquid melt.

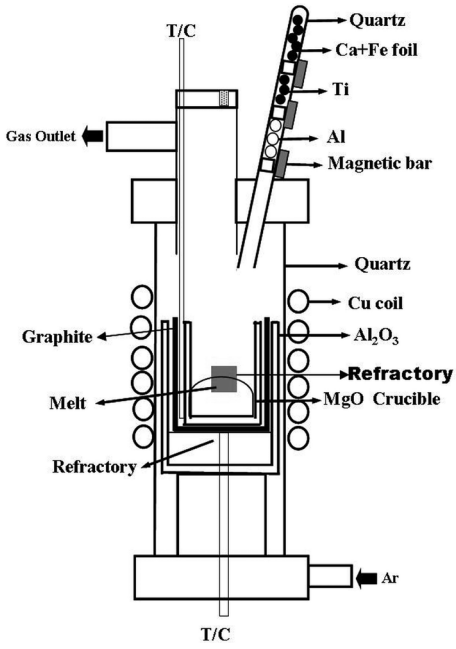

Figure 1: Schematic diagram of experimental induction furnace

The quenched sample was sliced into a plate shape and then sectioned to small pieces for analysis. The Ca, Mg and other elements were measured by inductively coupled plasma emission spectrometry. Total oxygen and nitrogen were analyzed by inert-gas fusion infrared absorptiometry. The shape of inclusions was monitored using SEM (Scanning Electron Microscope) and their compositions were determined by EDS (Energy-Dispersive Spectrometry).

RESULTS AND DISCUSSION

The experimental data of the effect of Ti on the dissolved amount of Mg or Ca in liquid iron at 1873 K are listed in Table 2. The liquid Mg and Ca temperature (T_{Mg}, T_{Ca}), which is maintained constantly for the Fe-Ti-Mg (or Ca) system, is also shown in Table 2.

The temperature dependence of the saturated vapor pressure of Mg or Ca is given by [16, 17],

$$\log P_{Mg} = 12.79 - 1.41 \log T_{Mg} - 7750/T_{Mg} [16] \quad (1)$$

$$\log P_{Ca} = 8.34 - 9670/T_{Ca} [17] \quad (2)$$

where P_{Mg} or P_{Ca} is in mmHg and T_{Mg} or T_{Ca} is in deg Kelvin. First, the dissolved contents of Mg in the binary Fe-Mg solution and the ternary Fe-Ti-Mg solution for the same P_{Mg} in the Mo chamber were determined. Since all of the binary and ternary iron melts saturated with Mg were under the same P_{Mg},

$$f'_{Mg}[\%Mg]' = f_{Mg}[\%Mg] \quad (3)$$

where, f'_{Mg} and f_{Mg} are the activity coefficients of Mg with respect to the 1% standard state based on Henry's law for the Fe-Mg solution and the Fe-Ti-Mg solution, respectively, $[\%Mg]'$ and $[\%Mg]$ are the saturated dissolved contents of Mg in iron melts for the Fe-Mg solution and the Fe-Ti-Mg solution, respectively.

$$f^{i}_{Mg} = f_{Mg}/f'_{Mg} = [\%Mg]'/[\%Mg] \tag{4}$$

According to $\lim_{[\%i]\to 0}\left(\partial \log f^{i}_{Mg} / \partial[\%i]\right)_{a'_{Mg}=a_{Mg}} = e'^{i}_{Mg}$,

$$e'^{i}_{Mg} = -\lim_{[\%i]\to 0}\left(\partial \log [\%Mg]' / \partial[\%i]\right)_{a'_{Mg}=a_{Mg}} \tag{5}$$

By plotting –log [Mg mass pct] against [Ti mass pct] in Table 2 and making a linear regression in the form –log [Mg mass pct] = A + e'^{Ti}_{Mg} mass pct Ti], the following regression equations and e'^{Ti}_{Mg} value was obtained. Similar to the preceding derivation, e'^{Ti}_{Ca} value was also obtained. The resultant regression line for Fe-Ti-Mg (or Ca) system, from which the values of e'^{Ti}_{Mg} and e'^{Ti}_{Ca} can be determined, is shown in Figure 2.

Using the relationship $e^{Ti}_{i} = e'^{Ti}_{i}\,(1 + 2.30[\%i]'e^{i}_{i})$, $i = Mg, Ca$ [18], the values of e^{Ti}_{Mg} and e^{Ti}_{Ca} can be evaluated. Since e^{Mg}_{Mg} or e^{Ca}_{Ca} are relatively small and [Mg mass pct] or [Ca mass pct] are also of order of magnitude of 10^{-3}, the term $2.30[\%Mg]'e^{Mg}_{Mg}$ or $2.30[\%Ca]'e^{Ca}_{Ca}$ can be ignored.

Thus,

$$e^{Ti}_{Mg} = e'^{Ti}_{Mg} \quad \text{and} \quad e^{Ti}_{Ca} = e'^{Ti}_{Ca} \tag{6}$$

From these result, the e^{Mg}_{Ti} value is negative, indicating that the employed solutal element Ti has a thermodynamic potential to decrease the activity coefficient of Mg in liquid iron. Such element could accelerate Mg dissolution into molten steels from slag or MgO-bearing refractory materials and play a role in favoring the formation of spinel inclusions.

Table 2: The equilibrium composition of metal sample and liquid Mg or Ca temperature

Fe-Mg-Ti system (T_{Mg}=1059 K)		
Ti(mass pct)	**Mg(mass pct)**	**-log[Mg mass pct]**
0.1800	0.0013	2.8861
0.9000	0.0170	1.7696
0.9400	0.0190	1.7212
1.0900	0.0170	1.7696
1.2200	0.0240	1.6198
1.2700	0.0290	1.5376
1.5323	0.0395	1.4034
Fe-Ca-Ti system (T_{Ca}=1438 K)		
Ti(mass pct)	**Ca(mass pct)**	**-log[Ca mass pct]**
0.2138	0.0027	2.5686
0.4243	0.0029	2.5376
0.5932	0.0033	2.4815
0.8042	0.0028	2.5528
0.9873	0.0036	2.4437
1.2342	0.0036	2.4437

1.9800	0.0043	2.3665
2.2100	0.0046	2.3372

Therefore, Ti is considered to be a significantly influential element in spinel formation (e^{Ti}_{Mg} = –0.933). A similar result was reported in previous work [19] investigating the composition and morphology changes of deoxidation products in the slag/metal (Fe-16pct Cr)/MgO crucible system.

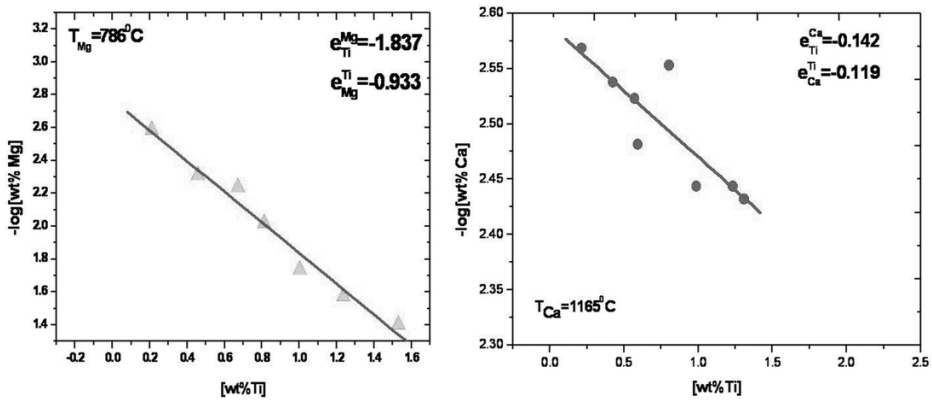

Figure 2: Regression lines according to above equations for Fe-Ti-Mg (or Ca) system

Figure 3 shows the types of inclusions in steel observed with the help of scanning electron microscopy. In the case of Ti addition, the initially formed FeO-Al_2O_3 inclusion was transformed to Al_2O_3-SiO_2 and subsequently to spinel, whereas Al_2O_3-SiO_2 remained as a stable inclusion for Si-Al deoxidation. Therefore, Ti should be added by careful attention to prevent of spinel formation in the production of high-grade clean steels when Ti is added.

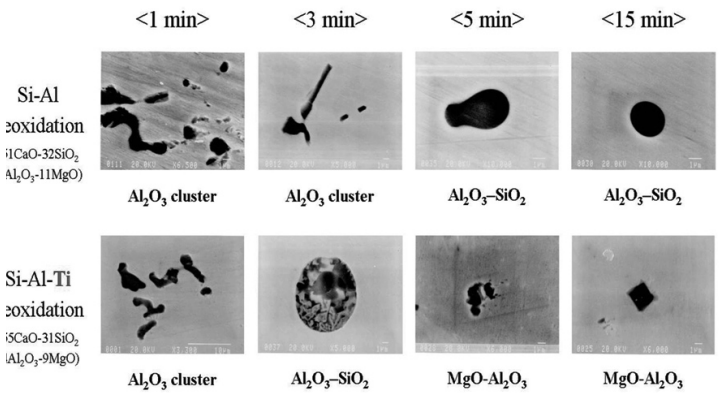

Figure 3: The variation of inclusion composition after deoxidation of Fe-16 mass pct Cr [19]

In a fashion similar to Fe-Ti-Mg ternary system, for the Fe-Ti-Ca ternary system, the resultant regression line for Fe-Ti-Ca system, from which the values of e^{Ti}_{Ca} can be determined, is shown in Figure 2. But, from previous and present results, the magnitude of interaction parameter between Ti and Mg are one order higher than those between Ti and Ca. Therefore, in this work, e^{Ti}_{Mg} was taken into account considering formation of inclusions.

First, austenitic stainless steel was deoxidized with Al. Then, Ti alloying addition was followed for austenitic stainless grade process. Finally, for modification of inclusions such as alumina and spinel, it was treated by Ca addition (ATC procedure). But, from above thermodynamic assessment, Ti alloying addition could accelerate Mg dissolution into molten steels from slag or MgO-bearing refractory materials. Thus, dissolved Mg combined with Al_2O_3 forms spinel inclusion in steels. Therefore, to reduce formation of spinel inclusions, Ca treatment method before Ti alloying addition could be considered (ACT procedure). In present work, the exchange of order between Ti addition and Ca treatment could examine its effectiveness by using induction furnace. A typical example of the variations of the melt compositions is shown in Figure 4. Mg and Ca contents increased right after Al deoxidation. Especially, the content of Mg increased right after Ti addition again in ATC procedure. However, in ACT procedure, Ca treatment suppressed the increasing dissolution of Mg. From this result, Ti alloying addition confirmed acceleration of Mg dissolution into molten steels from MgO-bearing refractory.

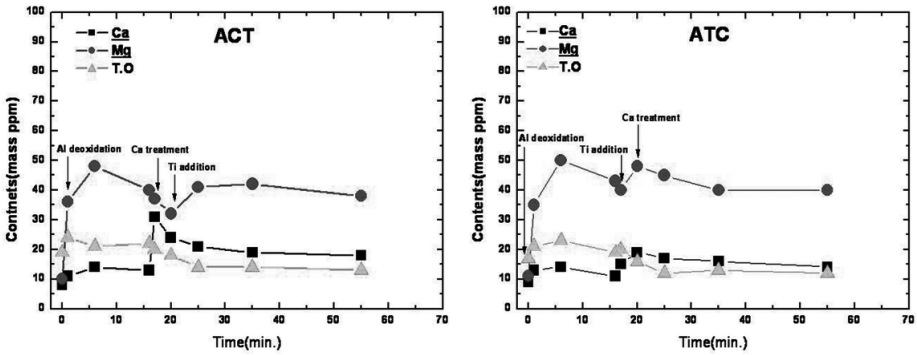

Figure 4: An example of variation of composition in ATC and ACT procedure

From compositional and morphological standpoint of inclusions, spinel inclusion which is induced dissolved Ti contents is observed obviously. From Figure 5, the typical variation of composition and morphology of inclusions is shown. In both procedure (ATC and ACT), after Al deoxidation, alumina inclusions that formed at the earliest stage of deoxidation showed the morphological feature of a cluster. But, in ATC procedure, after Ti alloying addition, typical spinel inclusions which exhibited angular-shaped tendency appeared.

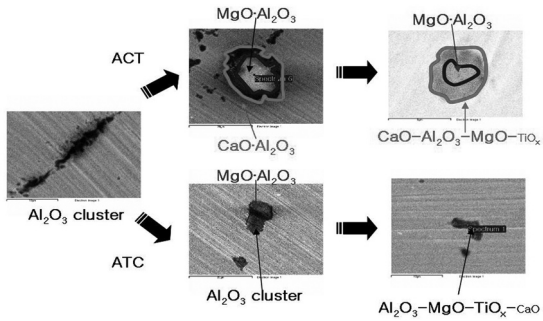

Figure 5: The variation of inclusion composition and morphology in ATC and ACT procedure

Thereafter, even though Ca treatment was conducted, these spinel inclusions are remained without modification of morphology occasionally.

On the other hand, in the case of the experiments in which Ca was added after the Ti addition, spinel inclusions surrounded by calcium aluminate which is globular were observed. As shown in Figure 6 calcium aluminates which are completely globular also were observed frequently in ACT procedure.

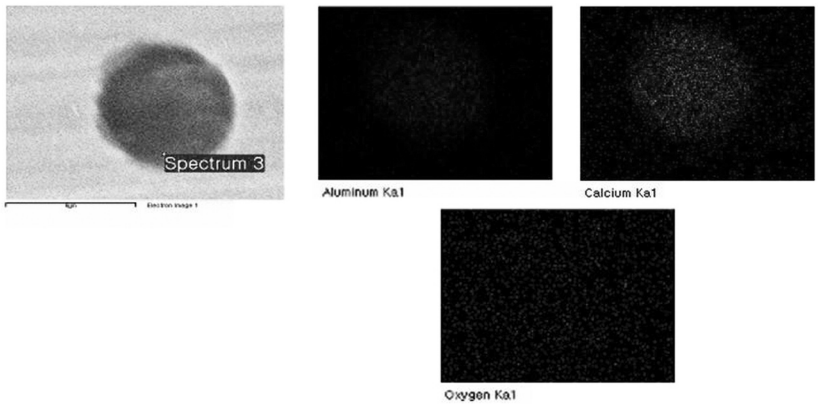

Figure 6: Element distributions of calcium aluminate inclusions in ACT procedure

In the present results, the activity of alumina can be approximated as one because the formed alumina was a pure product. Immediately, after adding Al to the melt, inclusion compositions were determined to consist of pure alumina. As previously mentioned, Mg contents were significantly increased after Ti addition. This implies that Mg dissolution simultaneously occurred as soon as Ti was added. The next step was that dissolved Mg reacted with alumina inclusions, which formed immediately after deoxidation with Al, resulting in the formation of spinel inclusions.

On the other hand, after Al deoxidation Ca treatment forms low melting calcium aluminate inclusions. That is, even if Mg has its higher activity than Ca in the melt, in a quantitative respect, Ca is more advantageous than Mg. Thus, alumina inclusions whose activity is higher reacted with Ca and changed to calcium aluminate inclusions.

CONCLUSIONS

For modification and prevention of inclusions, the effect of change of order between Ti alloying addition and Ca treatment was assessed. To clarify the thermodynamic role of Ti in steels, the interaction parameters between Mg (or Ca) and Ti were determined using the vapor/liquid equilibration method at 1873 K. The thermodynamic data at 1873 K determined in this work are the following:

$$e_{Mg}^{Ti} = -0.933,\ e_{Ca}^{Ti} = -0.119 \tag{7}$$

Considering the higher negative value of e_{Ti}^{Mg} than e_{Ti}^{Ca}, which suggests Ti has a significant thermodynamic potential to accelerate Mg dissolution from refractory. Thus, after Ti addition Ca treatment (ATC) was not recommended for the prevention of spinel formation.

After Al deoxidation, pure alumina inclusions formed. Thus, the activity of alumina is nearly one. Ti addition accelerated dissolution of Mg from refractory material into molten steel so that spinel inclusions formed easily. After that, the driving force for formation of calcium aluminate was weak because the activity of alumina was smaller than one.

On the other side, in ACT procedure, the pre-formed alumina inclusions reacted with early added calcium, effectively. Because of the reduced driving force of alumina inclusions ($a_{Al_2O_3}$ <1) to react and quantitative diminution, the formation of spinel inclusions was delayed and suppressed.

REFERENCES

JIS Handbook, Japanese Standards Association (2001). Tokyo, 2001, Vol. 1, p. 404. [1]

Itoh, H., Hino, M. & Ban-ya, S. (1998). Tetsu-to-Hagane, Vol. 84, pp. 90-98. [2]

Ohta, H. & Suito, H. (1997). Metall. Trans. B., Vol. 28B, pp. 1131-1139. [3]

Nishi, T. & Shinme, K. (1998). Tetsu-to-Hagane, Vol. 84, pp. 837-843. [4]

Okuyama, G., Takeuchi, S. & Sorimachi, K. (1997). CAMP-ISIJ, Vol. 10, p. 847. [5]

Kim, J. W., *et al.* (1996). ISIJ Int., Vol. 36, pp. S140-S143. [6]

Sigworth, G. K. & Elliott, J. F. (1974). Met. Sci., Vol. 8, pp. 298-310. [7]

Nadif, M. & Gatellier, C. (1986). Rev. Metall.-CIT, May, pp. 377-394. [8]

Turkdogan, E. T. (1996). *Fundamentals of Steelmaking.* The Institute of Materials, London, p. 121. [9]

Han, Q. (1990). Proceedings of the Sixth International Iron and Steel Congress, ISIJ, Nagoya, Japan, Vol. 1, pp. 166-176. [10]

Jo, S. J., Song, B. & Kim, S. H. (2000). Metall. Mater. Trans. B, vol.31B, pp. 1323-1332. [11]

Seo, J. D. & Kim, S. H. (2000). Steel Res., Vol. 71, pp. 101-106. [12]

Turkdogan, E. T. *Fundamentals of Steelmaking.* The Institute of Metals. [13]

Hayashi, Y., *et al.* (1990). Proceedings of the Sixth International Iron and Steel Congress, ISIJ, p. 551. [14]

Seo, J. D. & Kim, S. H. (1999). Bull. Kor. Inst. Met. Mater., Vol. 12, pp. 402-410. [15]

Zhang, X., Han, Q. & Chen, D. (1991). Metall. Trans. B, Vol. 22B, pp. 918-921. [16]

Rudberg, E. (1934). Phys. Rev., Vol. 18, p. 362. [17]

Fuwa, T. & Chipman, J. (1959). Trans, AME, Vol. 215, p. 708. [18]

Jeong, H. J. (2001). Master's Thesis, Pohang University of Science and Technology, Pohang, Korea. [19]